Optimal Lockdown in a Commuting Network
Online Appendix

Pablo D. Fajgelbaum, Amit Khandelwal, Wookun Kim, Cristiano Mantovani, Edouard Schaal

A Numerical Implementation

This section describes how the optimal planning problem is numerically implemented.

A.1 Optimal control problem

Assuming that the matching function is $M_j\left(\tilde{I},\tilde{S}\right)=\beta_j\tilde{I}\tilde{S}$, the optimal control problem (11) simplifies to

$$W=\max_{\boldsymbol{\chi}(t)}\int_0^\infty e^{-(r+\nu)t}\sum_j\left[U\left(j,t\right)+\frac{\nu}{r}\overline{U}\left(j,t\right)-\omega\gamma_D I\left(j,t\right)\right]dt$$

subject to

$$\dot{\mathbf{S}}\left(t\right)=-\mathbf{S}\left(t\right)\cdot\left[\mathbf{H}_S\left(t\right)'\operatorname{diag}\left(\boldsymbol{\beta}\right)\mathbf{H}_I\left(t\right)\mathbf{I}\left(t\right)\right] \tag{A.1}$$

$$\dot{\mathbf{E}}\left(t\right)=-\dot{\mathbf{S}}\left(t\right)-\gamma_I\mathbf{E}\left(t\right) \tag{A.2}$$

$$\dot{\mathbf{I}}\left(t\right)=\gamma_I\mathbf{E}\left(t\right)-\left(\gamma_R+\gamma_D\right)\mathbf{I}\left(t\right) \tag{A.3}$$

$$\dot{\mathbf{R}}\left(t\right)=\gamma_R\mathbf{I}\left(t\right) \tag{A.4}$$

and

$$\begin{aligned}U\left(j,t\right)&=U\left(j;\mathbf{S}\left(t\right),\mathbf{E}\left(t\right),\mathbf{I}\left(t\right),\mathbf{R}\left(t\right),\boldsymbol{\chi}\left(t\right)\right)\\ \overline{U}\left(j,t\right)&=U\left(j;0,0,0,\mathbf{S}\left(t\right)+\mathbf{E}\left(t\right)+\mathbf{I}\left(t\right)+\mathbf{R}\left(t\right)\right).\end{aligned}$$

The present-value hamiltonian can be written

$$\begin{aligned}H\left(t\right)=\sum_j\Bigg[&U\left(j,t\right)+\frac{\nu}{r}\overline{U}\left(j,t\right)-\omega\gamma_D I\left(j,t\right)\\&+\mu_S\left(j,t\right)\dot{\mathbf{S}}\left(j,t\right)+\mu_E\left(j,t\right)\dot{\mathbf{E}}\left(j,t\right)+\mu_I\left(j,t\right)\dot{\mathbf{I}}\left(j,t\right)+\mu_R\left(j,t\right)\gamma_R\mathbf{I}\left(j,t\right)\Bigg],\end{aligned}$$

where $\boldsymbol{\mu}_u$, $u=S,E,I,R$, are $J\times 1$ vectors of costate variables associated to each sickness status.

The first-order conditions of the problem are

$$[\mathbf{S}(t)] \quad \left(D_{\mathbf{S}}\mathbf{U}(t)+\frac{\nu}{r}D_{\mathbf{R}}\overline{\mathbf{U}}(t)\right)'\mathbf{1}_{J\times 1}+\operatorname{diag}\left(\mathbf{H}_S(t)'\operatorname{diag}(\boldsymbol{\beta})\mathbf{H}_I(t)\mathbf{I}(t)\right)(\boldsymbol{\mu}_E(t)-\boldsymbol{\mu}_S(t)) \tag{A.5}$$
$$=-\dot{\boldsymbol{\mu}}_S(t)+(r+\nu)\boldsymbol{\mu}_S(t)$$

$$[\mathbf{E}(t)] \quad \left(D_{\mathbf{E}}\mathbf{U}(t)+\frac{\nu}{r}D_{\mathbf{R}}\overline{\mathbf{U}}(t)\right)'\mathbf{1}_{J\times 1}+\gamma_I(\boldsymbol{\mu}_I(t)-\boldsymbol{\mu}_E(t))=-\dot{\boldsymbol{\mu}}_E(t)+(r+\nu)\boldsymbol{\mu}_E(t) \tag{A.6}$$

$$[\mathbf{I}(t)] \quad \left(D_{\mathbf{I}}\mathbf{U}(t)+\frac{\nu}{r}D_{\mathbf{R}}\overline{\mathbf{U}}(t)\right)'\mathbf{1}_{J\times 1}-\omega\gamma_D\mathbf{1}_{J\times 1}$$
$$+\mathbf{H}_I(t)'\operatorname{diag}(\boldsymbol{\beta})\mathbf{H}_S(t)\operatorname{diag}(\mathbf{S}(t))(\boldsymbol{\mu}_E(t)-\boldsymbol{\mu}_S(t))$$
$$-(\gamma_R+\gamma_D)\boldsymbol{\mu}_I(t)+\gamma_R\boldsymbol{\mu}_R(t)=-\dot{\boldsymbol{\mu}}_I(t)+(r+\nu)\boldsymbol{\mu}_I(t) \tag{A.7}$$

$$[\mathbf{R}(t)] \quad \left(D_{\mathbf{R}}\mathbf{U}(t)+\frac{\nu}{r}D_{\mathbf{R}}\overline{\mathbf{U}}(t)\right)'\mathbf{1}_{J\times 1}=-\dot{\boldsymbol{\mu}}_R(t)+(r+\nu)\boldsymbol{\mu}_R(t) \tag{A.8}$$

$$[\chi_t(j,k)] \quad \frac{\partial H(t)}{\partial \chi_t(j,k)}=0 \tag{A.9}$$

A.2 Algorithm

We solve the optimal control problem using the following steps. Set the terminal period T to be a large number. Given some initial condition $\left\{\mathbf{S}^{(n)}(0),\mathbf{E}^{(n)}(0),\mathbf{I}^{(n)}(0),\mathbf{R}^{(n)}(0),\mathbf{D}^{(n)}(0)\right\}$,

1. Initialize $n:=1$. Guess the policy $\boldsymbol{\chi}^{(1)}(t)$ for $t=0\dots T$ at the first iteration.
2. Using $\boldsymbol{\chi}^{(n)}(t)$, solve the partial differential equations (A.1)-(A.4) forward using the Euler method to recover $\left\{\mathbf{S}^{(n)}(t),\mathbf{E}^{(n)}(t),\mathbf{I}^{(n)}(t),\mathbf{R}^{(n)}(t),\mathbf{D}^{(n)}(t)\right\}$ for $t=1\dots T$. Solve for the economic allocation and the corresponding Jacobian in each t as described in the subsection A.3.
3. Using $\boldsymbol{\chi}^{(n)}(t)$ and the disease states, solve the partial differential equations (A.5)-(A.8) of the costates $\{\boldsymbol{\mu}_S(t),\boldsymbol{\mu}_E(t),\boldsymbol{\mu}_I(t),\boldsymbol{\mu}_R(t)\}_{t=0}^{T-1}$ backward using the Euler method with terminal condition
$$\{\boldsymbol{\mu}_S(T),\boldsymbol{\mu}_E(T),\boldsymbol{\mu}_I(T),\boldsymbol{\mu}_R(T)\}=0.$$
4. Compute $\boldsymbol{\chi}^*(t)=\operatorname{argmax}_{\boldsymbol{\chi}}H^{(n)}(t;\boldsymbol{\chi})$ using a numerical optimizer. This step uses the analytical gradient for the trade model described in the next section.
5. Stop if $\left\|\boldsymbol{\chi}^{(n)}-\boldsymbol{\chi}^*\right\|<\varepsilon$. Otherwise, set $\boldsymbol{\chi}^{(n+1)}=\lambda\boldsymbol{\chi}^*+(1-\lambda)\boldsymbol{\chi}^{(n)}$ where $0<\lambda<1$, set $n:=n+1$ and return to step (2).

Computing the maximizer $\boldsymbol{\chi}^*(t)$ for all t is the most computationally expensive step. Computation times can be improved by sampling a smaller number of dates t_1,t_2...t_N and interpolating the policy between those dates.

A.3 Solving the General Equilibrium Trade Model

We use two methods to compute the solution of the general equilibrium trade model at different stages of the numerical optimization:

Exact Solution

When solving the SEIR model forward, we compute the exact general equilibrium solution of the trade model by iterating over $w(j,t)$ for each t on the goods market equilibrium equation given a distribution of the state variables. Specifically, combining (4) and (7) we obtain:

$$w(j,t)=\frac{\sum_k Y(k,t)\left(\frac{\tau(j,k,t)}{P(k,t)}\frac{w(j,t)}{z(j)}\right)^{1-\sigma}}{\sum_{u=S,E,I,R}\sum_k N_u(k,j,t)}. \tag{A.10}$$

Further using (5) and (9) we obtain a system for wages at time t of the form

$$w(j,t) = H_j(w(1,t),..,w(J,t),t) \tag{A.11}$$

where the operator $H_j(w_1,..,w_J)$ takes the form

$$H_j(w_1,..,w_J) = \left(\frac{1}{\sum_{u=S,E,I,R}\sum_{k'} N_u(k',j,t)} \sum_k \frac{\left(\frac{\tau(j,k,t)}{z(j)}\right)^{1-\sigma}}{\sum_i \left(\frac{\tau(i,k,t)}{z(i)} w_i\right)^{1-\sigma}} \sum_{u=S,E,I,R} \sum_{i'} N_u(k,i',t) w_k \right)^{\frac{1}{\sigma}} \tag{A.12}$$

where $N_u(i,j,t)$ is given by (6).

Gradients

When evaluating the Jacobians $D_u\mathbf{U}(t)$ and $D_u\overline{\mathbf{U}}(t)$ for $u = S,E,I,R$ or when maximizing the Hamiltonian, we linearize the trade model around a nonlinear solution (the equilibrium under the current $\boldsymbol{\chi}$ to evaluate the Jacobian and the current equilibrium with $\boldsymbol{\chi} = 1$ for the Hamiltonian maximization).

Solving for the linearized equilibrium solely requires inverting a matrix for which we have an analytical expression. Specifically, totally differentiating the equilibrium conditions given shocks to the bilateral flows $d\ln N_u(j,i)$ of type-u workers or changes in trade costs $d\ln\tau$, and dropping the time subscript to save notation, we obtain the following linear system

$$\begin{aligned}
d\ln Y &= \sum_u (s_R(u)\cdot d\ln N_u)\,1_{J1} + \sum_u s_R(u)\,d\ln w \\
d\ln w &= s_X d\ln Y - (s_X\cdot d\ln s_M)\,1_{J1} - \sum_u (s_W(u)\cdot d\ln N_u)'\,1_{J1} \\
d\ln P &= s_M' d\ln w + (s_M\cdot d\ln\tau)\,1_{J1} \\
d\ln s_M &= (1-\sigma)\,d\ln w\times 1_{1J} - (1-\sigma)\,1_{J1} d\ln P' + (1-\sigma)\,d\ln\tau
\end{aligned}$$

where the first line is the total differential of (5), the second line corresponds to (7), the third line differentiates the price index (9) and the last line is the changes in the expenditure share, and where we are using vector notation such that $[d\ln N_u]_{i,j} = N_u(i,j)$, $[d\ln Y]_j = d\ln Y(j)$, $[d\ln P]_j = d\ln P(j)$, $[d\ln w]_j = d\ln w(j)$, and $[s_M]_{ij} = s(i,j)$ is the expenditure share. In these expressions, we have also defined $[s_X]_{ij} = s_X(i,j)$, $[s_W(u)]_{ij} = s_W(u,i,j)$ and $[s_R(u)]_{ij} = s_R(u,i,j)$ such that $s_X(i,j) \equiv \frac{Y(j)s(i,j)}{w(i)\sum_{u=S,E,I,R}\sum_j N_u(j,i)}$ is location j share in i's sales, $s_W(u,i,j) = \frac{N_u(i,j)}{\sum_{u=S,E,I,R}\sum_k N_u(k,j)}$ is the fraction of j's efficiency units corresponding to type u commuters from i, and $s_R(u,i,j) = \frac{N_u(j,i)w(i)}{Y(j)}$ is the fraction of resident of j's income corresponding to commuters to i in type u.

We can summarize the expressions as a solution for wages as a function of expenditure shares and labor flows shares:

$$\begin{aligned}
d\ln w = \Omega_w^{-1}\Big[&\sum_u s_X\,(s_R(u)\cdot d\ln N_u)\,1_{J1} - (1-\sigma)\,s_X\,(s_M\cdot d\ln\tau)'\,1_{J1} \\
&+ (1-\sigma)\,(s_X\cdot d\ln\tau)\,1_{J1} - \sum_u (s_W(u)\cdot d\ln N_u)'\,1_{J1}\Big]
\end{aligned} \tag{A.13}$$

where

$$\Omega_w = I_J - \sum_u s_X s_R(u) - (1-\sigma)\,\mathrm{diag}(s_X 1_{J1}) + (1-\sigma)\,s_X s_M'. \tag{A.14}$$

The gradients with respect to χ, S, E, I and R then follow using the definition of $N_u(i,j)$ in (6).

B Relationship between Commuting and Infections

We follow Fang et al. (2020) to assess the relationship between new daily infections and 21-day lags of commuting in a reduced form specification:

$$\ln(1 + \text{new cases}_{it}) = \alpha_i + \gamma_{city(i),t} + \sum_{k=0}^{21} \beta_k \ln(flow_{i,t-k}) + \epsilon_{it} \tag{A.15}$$

where α_i is a district fixed effect and $\gamma_{city(i),t}$ is a fixed effect that varies by city and date t. This specification flexibly controls for city-level trends due to forces other than commuting. It identifies the impact of flows from cross-sectional variation by exploiting a district's flows above or below its average. The variable $flow_{it}$ is either the total number of people who leave from district i (outflows) or arrive into district i (inflows). The specification pools over the three cities since number of districts in each city is small, but we weight the regression so that each city contributes equally. Standard errors are clustered by i using the block bootstrap to account for a small number of clusters (Cameron et al., 2008).

We do not have an instrument for commuting that varies across space, so the coefficients must be interpreted with caution. For example, changes in commuting may be correlated with behavioral changes. Figure A.4 reports the coefficients. It shows an inverted-U shape peaking between 8-15 days when looking at inflows. The p-value of the joint test $\beta_k = 0$ for $k = \{0, ..., 7\}$ is 0.040, for $k = \{8, ...15\}$ is 0.001, and for $k = \{16, ..., 21\}$ is 0.159. The results for outflows are noisier and we do not target these moments in the structural estimation, but they seem consistent with an incubation period after which people showing symptoms get tested or come to the hospital.

C Robustness of Optimal Lockdown Patterns

We implemented robustness with respect to key parameters, as described in Section 3.3. We consider a lower infection fatality ratio (0.03%); a faster recovery time (10 days); an estimation of the transmission rate starting at the peak of new cases; an asymptomatic rate of half the benchmark; a large shock such that 1% of the population is infected; twice the value of life of the benchmark; and a shorter incubation (4.1 days). Figure A.5 shows that the qualitative patterns of optimal lockdown from the benchmark are similar across these specifications, except for Seoul given a large shock, as previously mentioned. Doubling the value of life or introducing a large shock leads to stronger initial lockdown, in particular for central locations, while a lower death rate weakens it.

D Additional Tables and Figures

Table A.1: Commuter Data Summary Statistics

	Daegu	Seoul	NYC Metro
Population	2,438,031	9,729,107	19,467,622
# Districts	8	25	20
Sample Period	Jan 1, 2018–Apr 30, 2020	Jan 1, 2018–Apr 30, 2020	Jan 1, 2020–Apr 30, 2020
Data Source	Subway ridership	Subway/bus ridership	Mobile phones
Flow Type	Turnstile	Bilateral	Bilateral
First Case	Feb 17, 2020	Jan 30, 2020	Mar 3, 2020
Lockdown Date	Feb 24, 2020	Feb 24, 2020	Mar 22, 2020
# Cumulative Cases	6,778	354	389,603

Notes: Table reports summary statistics for the Daegu, Seoul, and NYC Metro data. Administrative units within the two Korean cities are called districts with an average population of 368,701 and an average land area of 45 km^2. Administrative units within NYC Metro are counties with an average population of 1,232,768 and an average land area of 690 km^2. Cumulative Covid-19 cases are as of April 30 2020.

Figure A.1: Bilateral Commute Flows and Expenditures

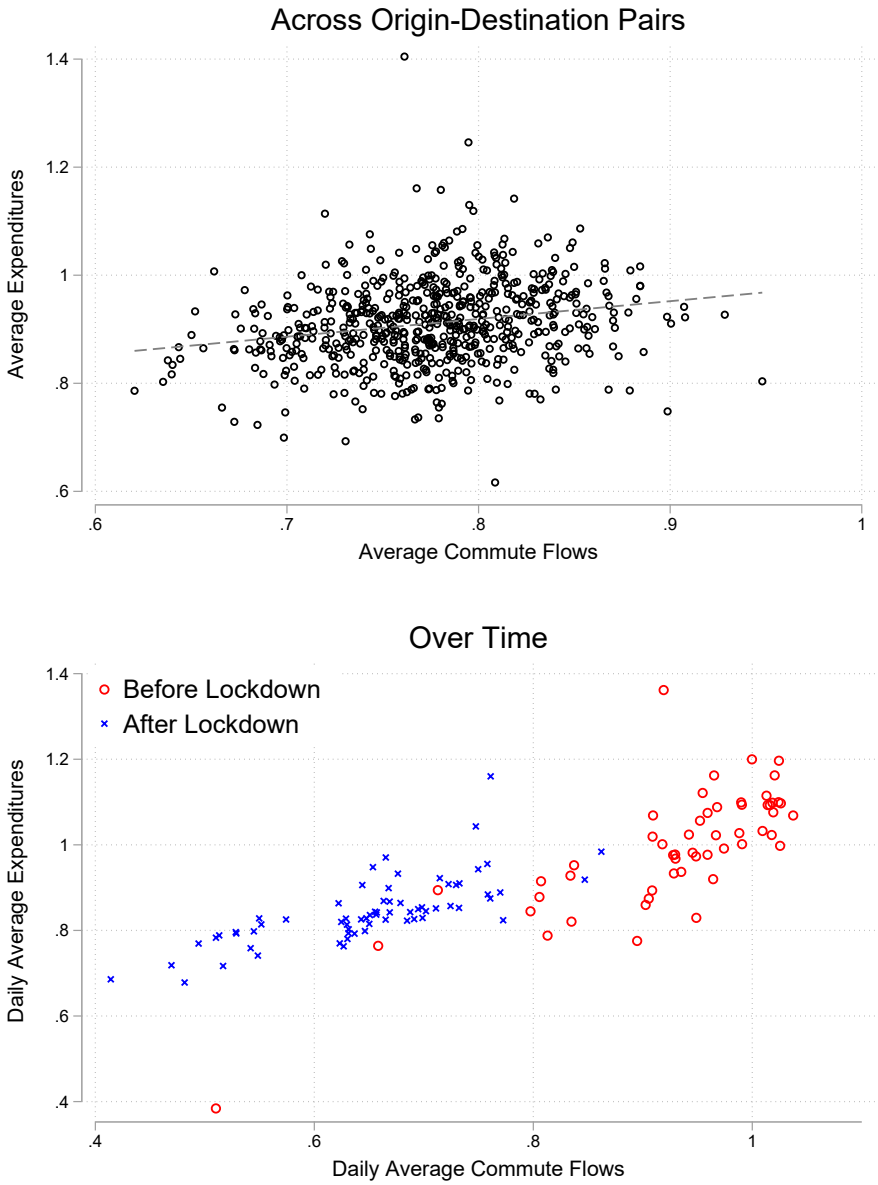

Note: Figure reports district-to-district expenditures against commute flows for Seoul, both normalized by their pre-pandemic levels. The top panel reports commute flows and expenditures for each of the 625 bilateral district pairs averaged over January 1 2020 to April 30 2020. The bottom panel reports commute flows and expenditures averaged across all 625 district pairs for each of the 121 days during this time period.

Figure A.2: New Cases per District: Data and Estimation

(a) Daegu (b) Seoul (c) NYC Metro

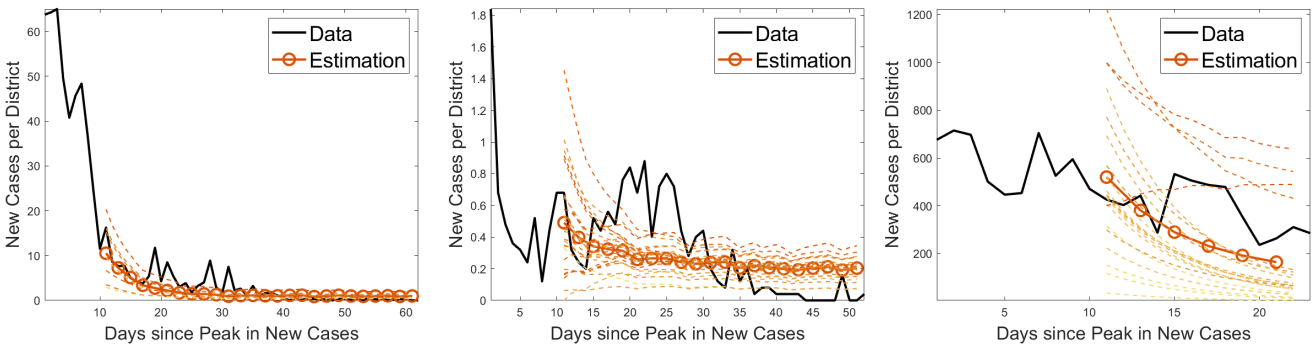

Note: The solid lines show the average number of new cases per district over time since the peak in new cases in the data. The dashed lines are the number of new cases by district in the estimated model corresponding to equation (18), assuming that commuting changed as observed in the data (the shade of the lines represent the share of commuter inflows, with darker shades representing more inflows). The calibration is implemented using case data starting 10 days after the peak in new cases in each city. The solid line with circle markers is the total case number per district in the estimated model.

Figure A.3: Optimal Lockdown over Districts and Time

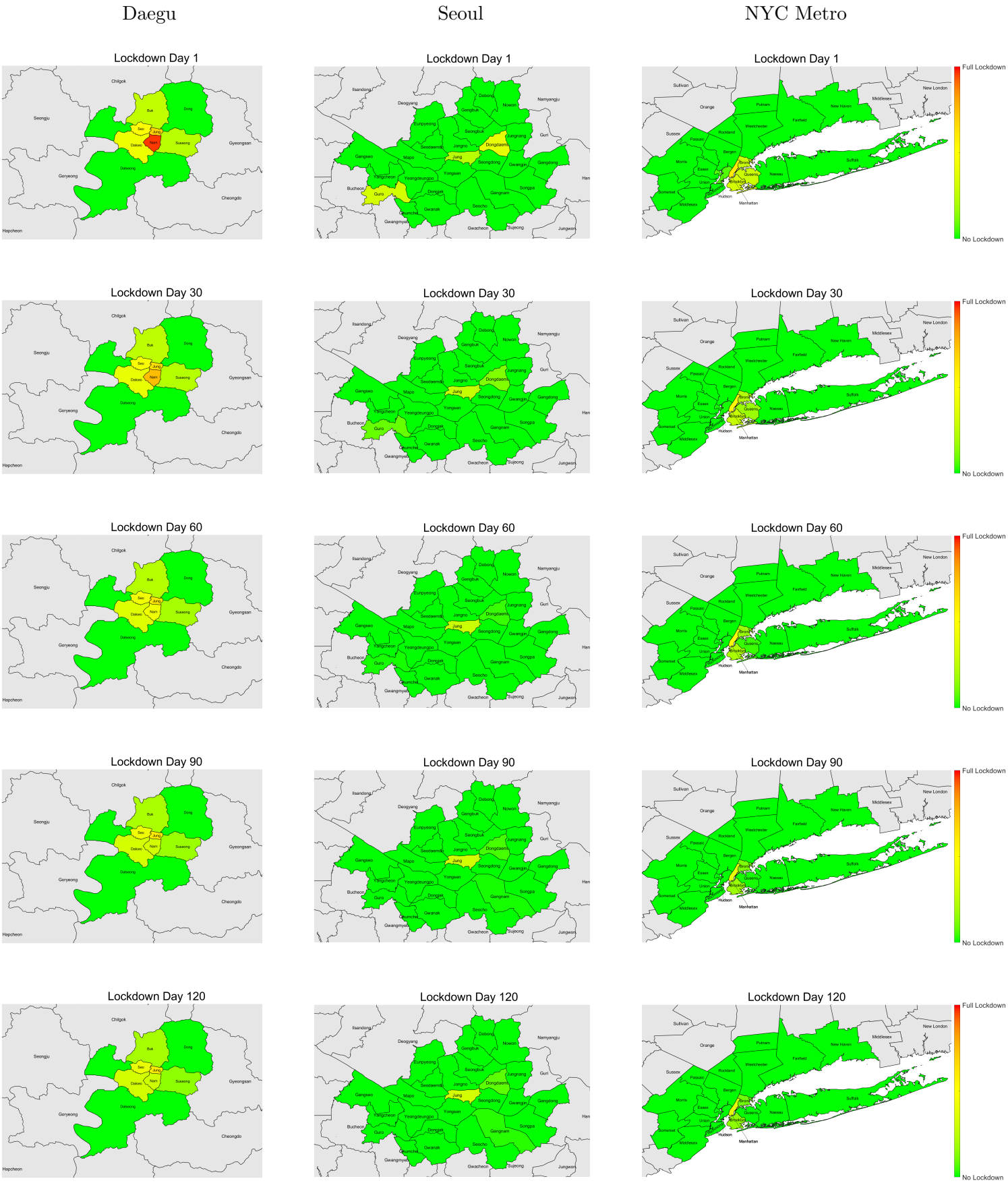

Note: The figure plots the optimal policy in the commuting area at different points in time. Redder colors denote more stringent lockdowns.

Figure A.4: Commuting and New Daily Cases

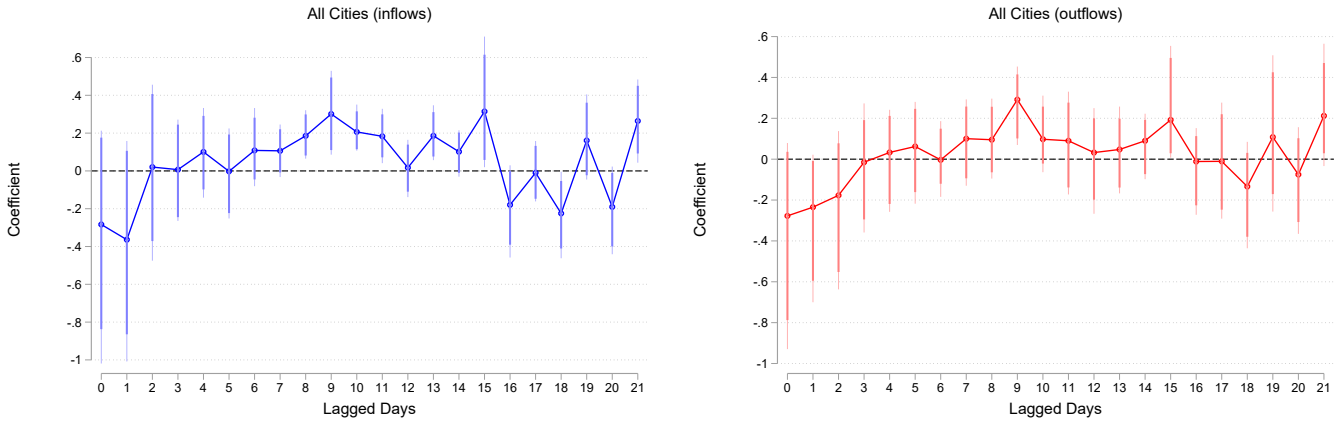

Note: The figure plots the coefficients from equation (A.15). The left panel reports results using inflows as the independent variable. The right panel reports outflows as the independent variable. The regression pools over the three cities and applies weights so that each city contributes equally. The regression uses data since January 22 2020. Error bars show 90 percent (thick) and 95 percent (thin) confidence intervals. Standard errors are clustered by using the block bootstrap to account for a small number of clusters.

Figure A.5: Robustness

(a) Daegu

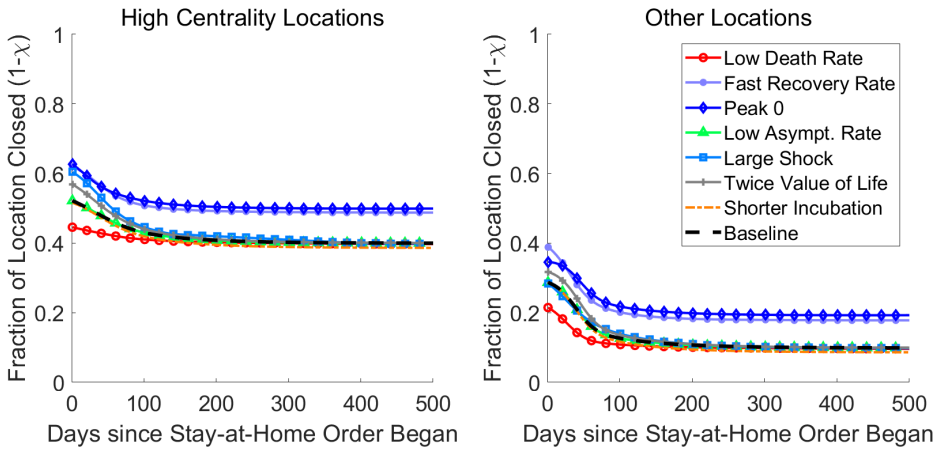

(b) Seoul

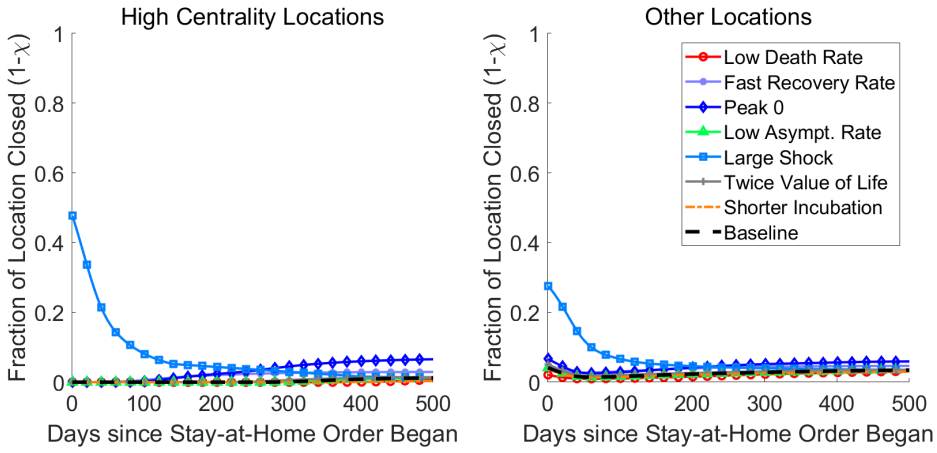

(c) NYC Metro

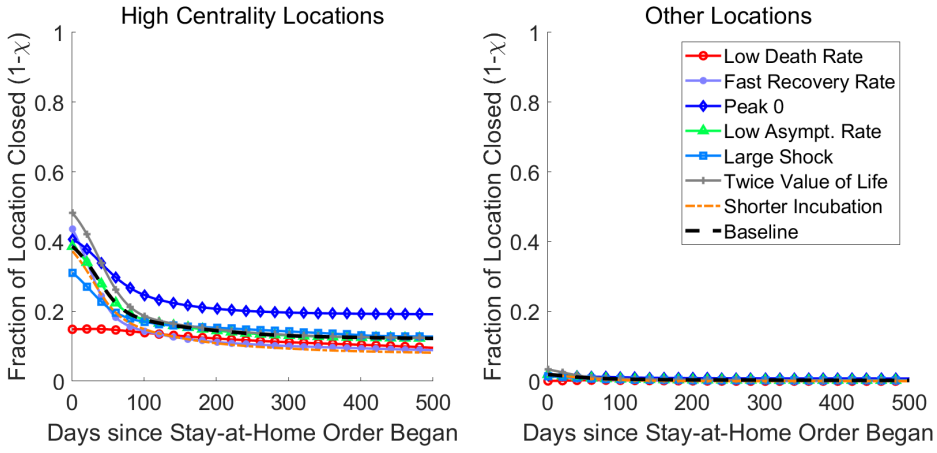

Note: Plotted optimal policies are defined as mean policy for high centrality vs other locations for each city. The different cases correspond to the alternative parametrizations described in Section 3.3 and discussed in Section C.

Figure A.6: Seoul: Optimal Lockdown in Baseline and Alternative Scenarios

(a) Baseline (b) Large Shock (c) High Value of Life

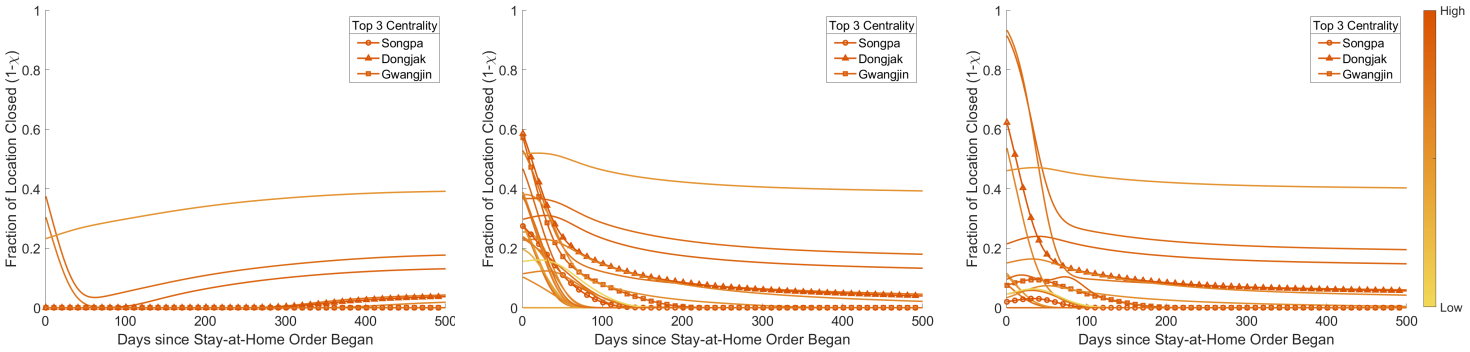

Note: The three panels show the results for Seoul under the baseline calibration (left panel), a large shock infecting 1% of the population (middle panel) and a value of life that is 100 times the benchmark (right panel).

Figure A.7: Centrality of Commuting Locations and Optimal Policies (Virus Diffusion through Shopping)

(a) Daegu

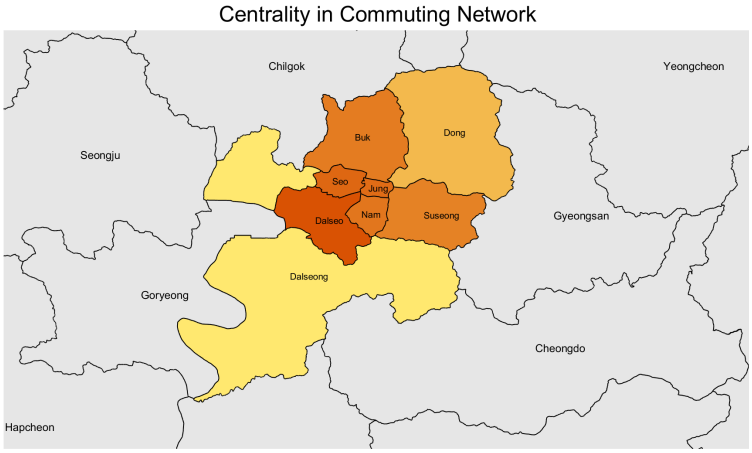

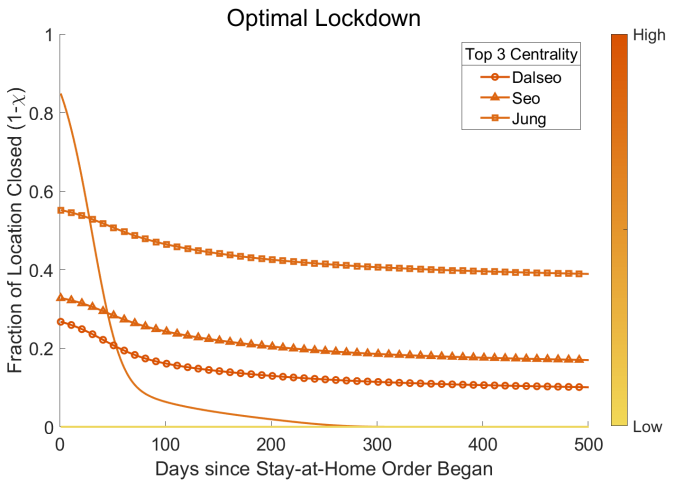

(b) Seoul

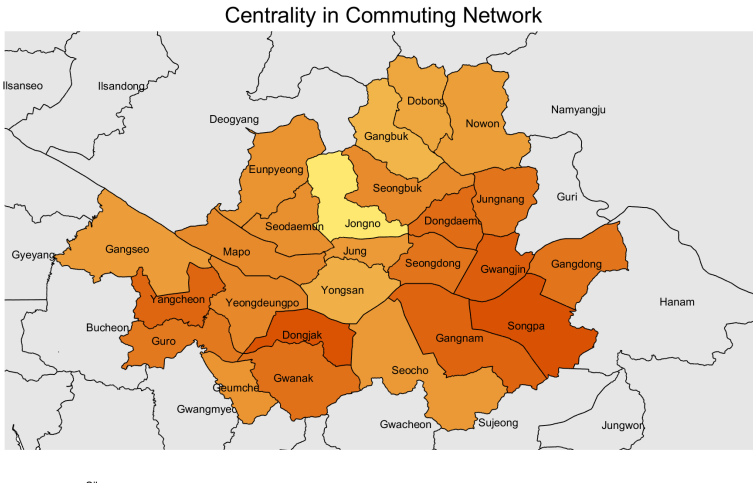

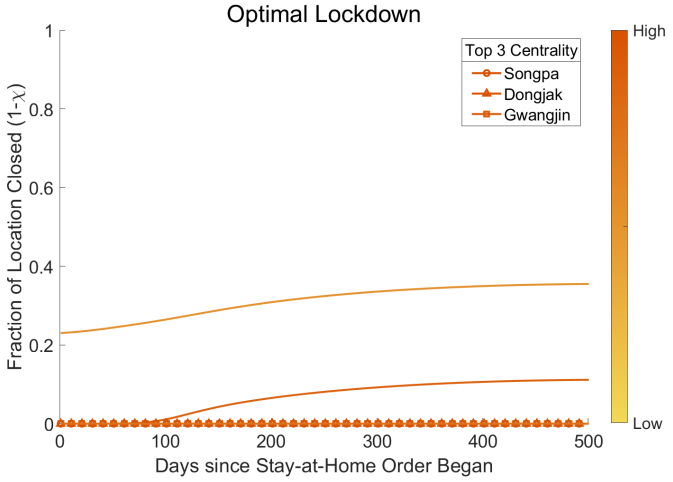

(c) NYC Metro

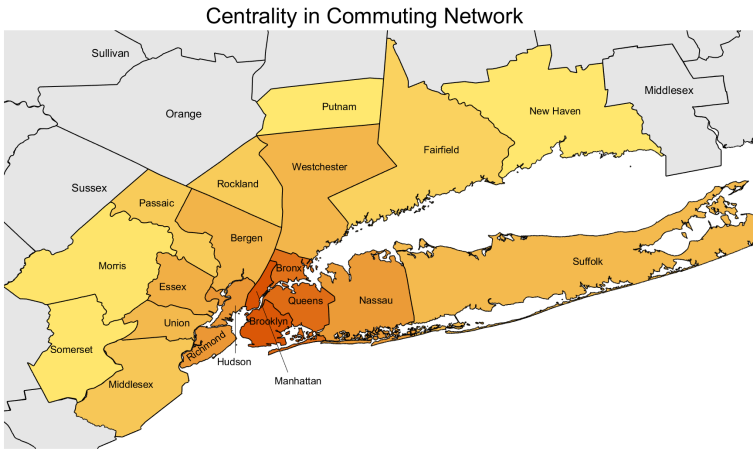

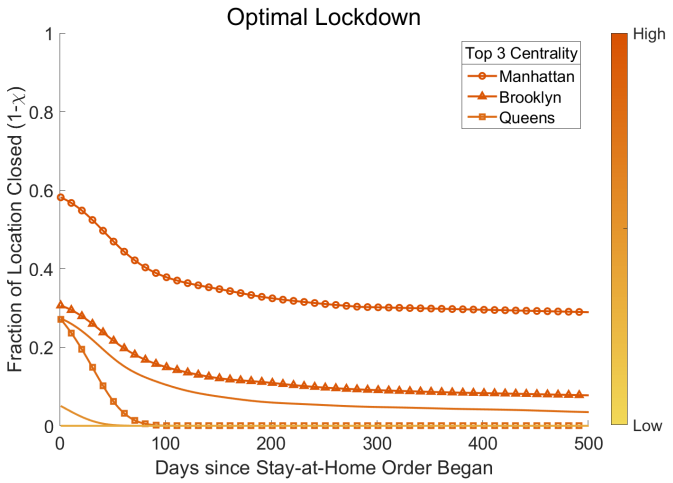

Note: The left panel denotes the (log) centrality of a location (see footnote 17), normalized so that the most central location is 1. The right panel plots the optimal policies over time for each location in the network. The color of the line represents the centrality of the location in the network. The three most central locations in the network are indicated in the legend.

Figure A.8: Pareto Frontiers (Virus Diffusion through Shopping)

(a) Daegu

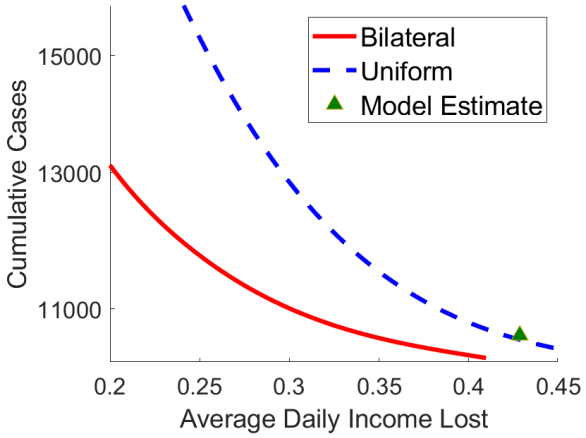

(b) Seoul

(c) NYC Metro

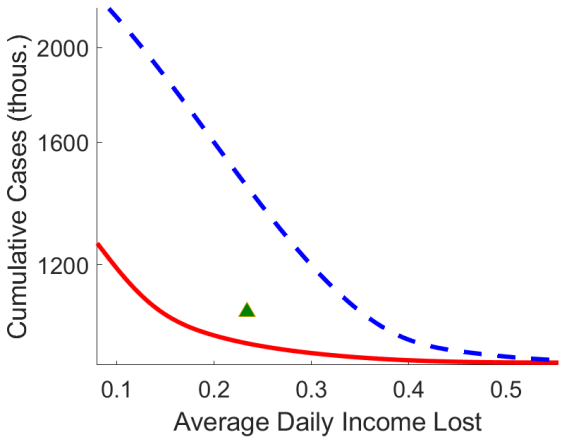

Note: The figures plot the cumulative number of new cases (y-axis, log scale) and the average real income lost per day between the date of the first confirmed case (see Appendix Table A.1) and April 30 2020 for parametrizations of the value of life (ω) ranging from 1/100 to 100 times the benchmark, in both the optimal lockdown with space and time variation ("Spatial") and in the spatially uniform optimal solution with time variation only ("Uniform", i.e., the same lockdown across all locations). The green triangle shows the case count and real income lost implied by the estimated model on April 30 2020.

Figure A.9: Changes in Commuting Flows: Optimal and Observed (Virus Diffusion through Shopping)

(a) Daegu

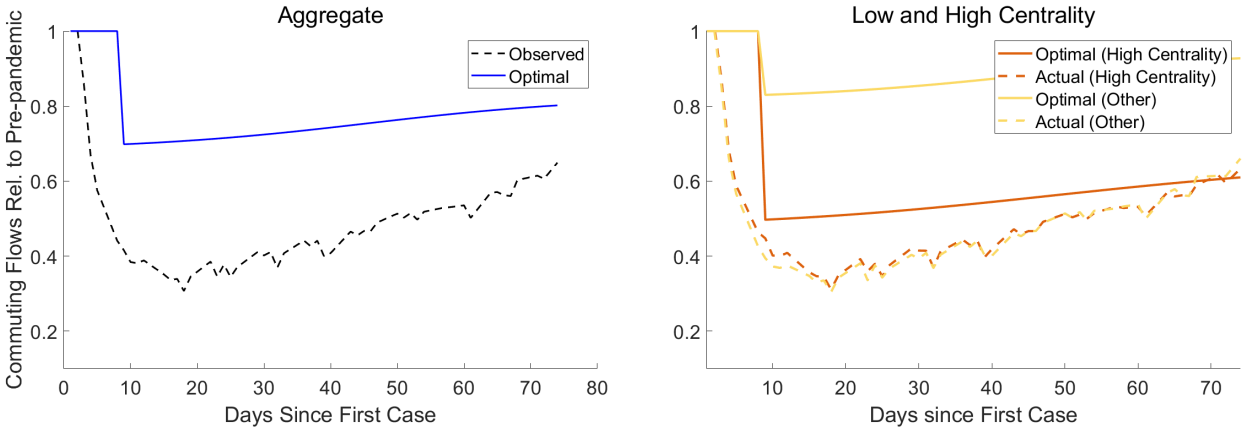

(b) Seoul

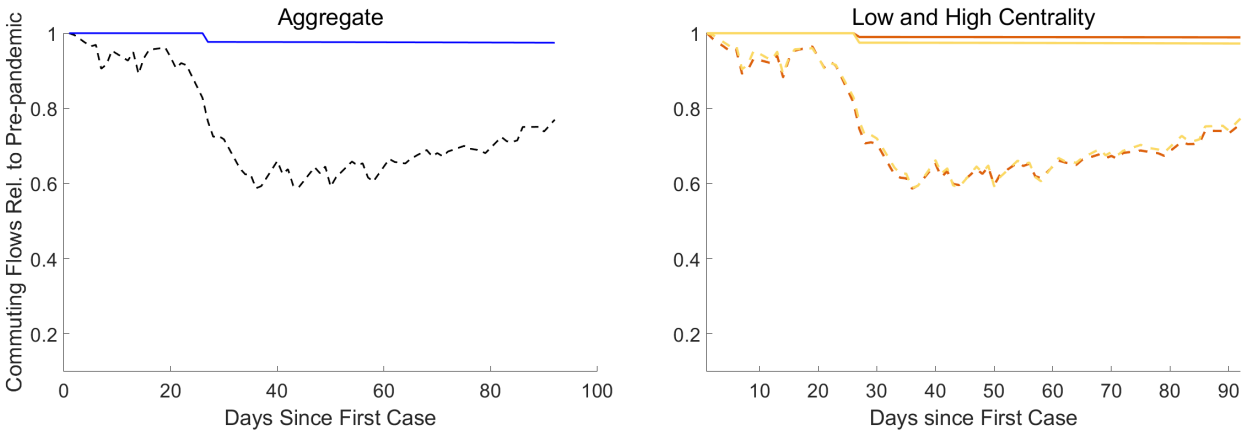

(c) NYC Metro

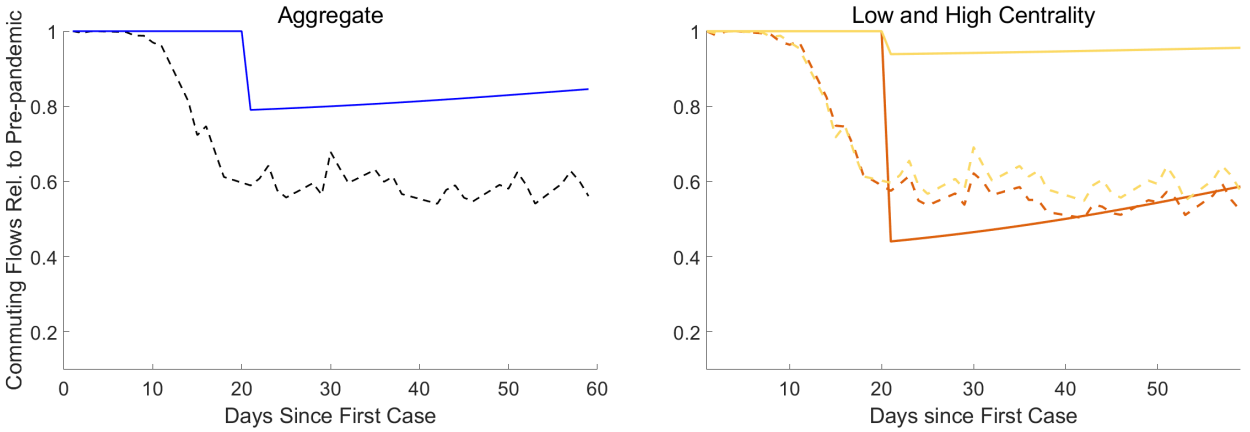

Note: In the left panel, the dashed black line shows the aggregate commuting flows in each city starting from the date of the first confirmed case in each city. The solid and circled blue lines show the aggregate commuting flows implied by the optimal spatial policy. In the right panel, optimal and observed commuting responses are divided by top-3 centrality locations (darker shade) and the other locations.